Turbulent drag reduction by the seal fur surface

Turbulent drag reduction by the seal fur surface

Motoyuki Itoh[a] and Shinji Tamano
Graduate School of Engineering, Nagoya Institute of Technology, Gokiso-cho, Showa-ku, Nagoya, Aichi 466-8555, Japan

Ryo Iguchi
Nippon Steel Corporation Yawata Works, Tobihata-cho, Tobata-ku, Kitakyushu 804-8501, Japan

Kazuhiko Yokota
Graduate School of Engineering, Nagoya Institute of Technology, Gokiso-cho, Showa-ku, Nagoya, Aichi 466-8555, Japan

Norio Akino
Institute for the 24th Century World, Second F CCI-building, 2-8-13 Kaimon-cho, Hitachinaka, Ibaraki 311-1222, Japan

Ryutaro Hino
Nuclear Science and Energy Directorate, Japan Atomic Energy Agency, 4002 Narita-cho, O-arai-cho, Higashi-ibaraki-gun, Ibaraki 311-1394, Japan

Shinji Kubo
Nuclear Science and Energy Directorate, Japan Atomic Energy Agency, Nuclear Applied Heat Transfer Division, IS Process Technology Group, 4002 Narita-cho, O-arai-cho, Higashi-ibaraki-gun, Ibaraki 311-1394, Japan

(Received 15 December 2005; accepted 24 April 2006; published online 8 June 2006)

The drag-reducing ability of the seal fur surface was tested in a rectangular channel flow using water and a glycerol-water mixture to measure the pressure drop along the channel in order to evaluate friction factors in a wide range of Reynolds number conditions, and the drag reduction effect was confirmed quantitatively. The maximum reduction ratio was evaluated to be 12% for the glycerol-water mixture. The effective range of the Reynolds number, where the drag reduction was remarkable, was wider for the seal fur surface compared to that of a riblet surface measured in this channel and in previous studies. It was also found that for the seal fur surface, unlike riblets, any drag increase due to the effect of surface roughness was not found up to the highest Reynolds number tested. Measurements of the seal fur surface using a 3D laser microscope revealed that there were riblet-like grooves, composed of arranged fibers, of which spacings were comparable to that of effective riblets and were distributed in various wavelengths. Using LDV measurements, it was found that the difference in the mean velocity scaled by the outer variable among the smooth, riblet, and seal fur surfaces did not appear at any spanwise locations. Streamwise turbulence intensity for the seal fur surface was found to be about 5% smaller than those for smooth and riblet surfaces.
 [DOI: 10.1063/1.2204849]

I. INTRODUCTION

It has been recognized that riblets[1–3] which consist of microgrooves or microfences on the bounding surface aligned with mean flow direction with small transverse spacing are one of the popular passive control methods used for a wall-bounded turbulent flow. It is well known that standard two-dimensional riblets have the ability to reduce friction drag up to 8% for the turbulent boundary layer.[1–3] In addition, a drag-reduction effect due to a riblet surface has also been found for internal flows such as turbulent channel flow[4,5] and pipe flow.[6–8] To clarify the drag reduction mechanism due to riblets, velocity measurements over riblet surfaces have been conducted using a hot-wire anemometer,[9–12] laser-Doppler velocimetry (LDV),[13–15] and particle image velocimetry (PIV).[16] These experimental studies and recent direct numerical simulations[17–19] of turbulent channel flow with riblet surfaces have provided a considerable amount of valuable knowledge on the mechanisms of drag reduction due to riblets. It has been widely accepted as a reasonable explanation that riblets work as a longitudinal fence to reduce skin-friction drag by impeding spanwise movement of longitudinal vortices during sweep events.[20]

Sirovich and Karlsson[21] reported that an aligned pattern of wall protrusions resulted in a drag increase in excess of 20%, while a simple change of pattern into random resulted in a drag reduction of up to 10%. This indicates that randomly patterned surfaces have the possibility to yield a higher drag reduction than two-dimensional riblets uniformly aligned with the streamwise direction. Recently, three-dimensional riblets, simulating the real scales of a fast shark, have been investigated to seek a higher drag reduction.[22,23] For engineering and industrial applications, new techniques

[a]Telephone: +81 52 735 5328. Fax: +81 52 735 5247. Electronic mail: itoh.motoyuki@nitech.ac.jp

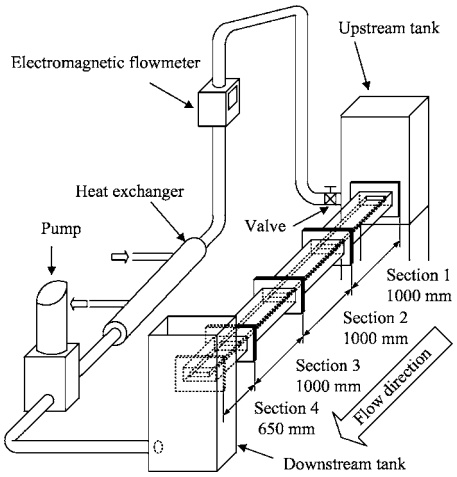

FIG. 1. Experimental apparatus.

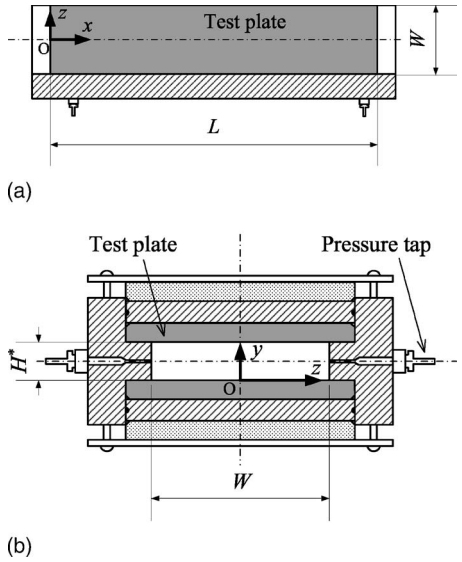

FIG. 2. Frame of reference: (a) x-z plane, (b) y-z plane.

are much needed to achieve the same or a higher turbulent drag reduction as an alternative to the two- or three-dimensional riblet. Hairy surfaces may be one of the promising candidates from the standpoint of seeking an idea from natural creatures such as the riblet which is an idealized model of shark skin.

In the present study, the pressure loss for seal fur surface was measured in a rectangular channel flow in order to reveal its drag-reducing ability. To evaluate the surface position under flowing conditions, the pressure loss in the laminar flow region was measured precisely using a glycerol-water mixture of which viscosity was larger than water. The seal fur surface looked furry and soft in a dry condition, but, in a wet condition, it became smooth and stiff by close attachment of each fiber of the seal fur onto the skin, aligned in one direction. Therefore, morphological observation and measurement of a seal fur surface in the wet condition was carried out using a three-dimensional laser microscope. In addition, mean velocity and streamwise turbulence intensity were measured using a LDV system. The results obtained for the seal fur surface were compared with the corresponding statistics for smooth and riblet surfaces.

II. EXPERIMENTAL APPARATUS AND PROCEDURE

The experiments were conducted in a rectangular channel made of acrylic resin with a channel width $W=140$ mm, nominal channel height $H^*=30$ mm, and total channel length of 3 650 mm consisting of four sections (see Fig. 1). The working fluids used were water and a glycerol-water mixture (40 wt. %). The glycerol-water mixture was used to measure pressure loss at the low Reynolds number precisely. The kinematic viscosity and specific gravity of the glycerol-water mixture were measured by a capillary kinematic viscometer and a Baume's hydrometer, respectively. The working fluids, with their temperature kept constant by a heat exchanger, were circulated by a centrifugal pump. The turbulence and spatial irregularities of the flow were reduced by passing through perforated plates in the upstream tank. The flow rate was controlled by the pump with an inverter power source and a valve, and measured by an electromagnetic flowmeter. The upstream two sections of channels 1 and 2 were in the developing region of 2 000 mm long, and the downstream section 3 was in the measuring region of 1 000 mm long. The channel-aspect ratio of the present duct was $W/H^*=4.67$. Dean[24] reported that three-dimensional effects disturbed the flow near the center plane if the aspect ratio was less than 7. Therefore, we investigated the effect of the secondary flow, which was one of the three-dimensional effects, on the velocity field. The upper and lower walls of section 3 were test plates of $900\times180\times15$ mm, which were convertible, while the side walls were fixed and smooth. In this study, x, y, and z represent the streamwise, wall-normal, and spanwise directions, and their origins are on the locations of the upstream end of the test plate, the lower wall surface, and the center of the channel, respectively (Fig. 2). Here L is the length of the test plate ($L=900$ mm).

Smooth and riblet surfaces made of acrylic resin plates and a set of plates adhered by sheets of seal furs were tested. The riblets were carved on the surface of the test plate. The cross section of the elemental rib of the riblet used was a trapezoid with bases of 0.35 mm and tops of 0.15 mm and the height $h=0.70$ mm (Fig. 3). The lateral rib spacing s was 0.70 mm, and thus the shape factor was $h/s=1$. Bechert *et al.*[5] reported that the trapezoidal groove riblet yielded the higher maximum drag reduction (8.2%), compared to the conventional riblet configurations with triangular and semi-

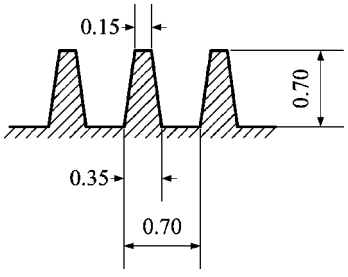

FIG. 3. Cross section of elemental rib of riblet (unit, mm).

circular grooves. The shape of the present riblet was measured by a three-dimensional laser microscope described below and is not sharp at the tops, which is different from that of Bechert *et al.*[5] The theoretical calculation of Bechert and Bartenwerfer[25] for riblet surfaces with rounded ridges suggests that the maximum drag reduction ratio of the present riblet surface should be smaller than that of Bechert *et al.*[5] A sheet of fur was cut out from a whole body skin of an adult ribbon seal along backbone choosing parts without hole, bold and irregular spots of hair. The direction of the seal hair was streamwise (x). The seal fur used was tanned by tannin, so the surface had a hydrophilic property and became wet easily in water. We confirmed that the hair of the seal fur was glued to the test surface during the experiments.

The friction factor was obtained by measuring the pressure loss between the locations at a streamwise interval of 800 mm in section 3. Two kinds of pressure transducers (GE Druck Co. Ltd., LPM5481 and Validyne Engineering Co. Ltd., DP15-20) whose full scales were 50 Pa and 600 Pa and linearity was ±0.25% were used for measurements of pressure loss. Measurements of the friction factor generally lead to a more accurate estimation of the drag-reduction ratio than the method using velocity measurements, which is why the present experiments were carried out for internal flow, i.e., rectangular channel flow, not for an external flow such as a boundary layer flow. Working fluids filling the rectangular channel were allowed to rest for more than 2 days to allow air bubbles to escape. We confirmed that the friction factors after 2 days were the same as those after 3 days (see Fig. 10 in detail). The temperature difference between before and after a test run was within ±0.1 °C.

The configuration of seal fur surface was measured by a three-dimensional laser microscope with a resolution of 0.02 μm. Measurement was done under a semiwet condition by the glycerol-water mixture rather than fully immersed conditions due to the measuring limitations of the laser microscope. Data samples numbered 20 000 in the spanwise length of 15 mm. We checked the measurement accuracy of the microscope under the semi-wet condition by measuring the riblet surface, and confirmed that its accuracy was adequate for the lateral spacing of riblets. Unfortunately, however, the accuracy of the depth measurement here was insufficient because of the effect of the glycerol-water mixture remaining in the bottom of riblets.

A LDV system (300 mW argon-ion laser) was used in the backscatter mode. Laser light was passed through the side of the channel. The LDV probe was slightly tilted (5°) with respect to the test plate surface in order to measure velocity very close to the wall. The probe was traversed in three orthogonal directions at a resolution of 0.01 mm using a traversing mechanism. Flow was seeded with nylon powder particles (mean diameter, 4.1 μm and specific gravity, 1.02). LDV measurements were made at the spanwise locations of $z/W=0$, 0.22, 0.38, 0.42, and at the streamwise locations $x/L=0.89$ ($x=800$ mm). Velocity measurements were carried out at the Reynolds number $\mathrm{Re}_m=7\,000$ for the water and glycerol-water mixture. Typical data rates in the locations away from the wall were about 400 Hz, falling off to about 10 Hz very close to the wall ($y\simeq 0.05$ mm). Data samples for each location were more than 10 000.

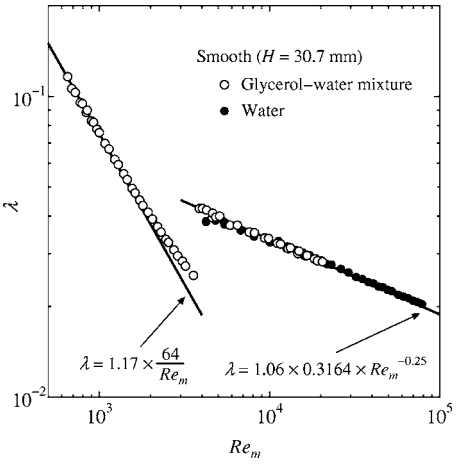

FIG. 4. Friction factor versus Reynolds number on the smooth surface.

III. RESULTS AND DISCUSSION

A. Effective channel height

We cannot directly measure the channel height, the distance between the upper and lower plates for the riblet and seal fur surfaces, where the channel height is not constant due to the roughness of the protrusions and recessions. For an accurate evaluation of friction factors, it is essential to estimate the channel height as exactly as possible, since the friction factor evaluated varies approximately with the cube of a channel height for the duct flow. Hence, the effective channel height H was introduced and defined as the distance between the upper and lower plates at which the measured friction factor agreed with the laminar theoretical relation between the friction factor λ and the Reynolds number Re_m for a smooth surface in the laminar flow region ($\mathrm{Re}_m < 1\,500$). The Reynolds number Re_m is defined as follows:

$$\mathrm{Re}_m = \frac{d_h U_a}{\nu}, \tag{1}$$

where $d_h = 2HW/(H+W)$ is the equivalent diameter (W is the channel width=140 mm), $U_a = Q/(HW)$ is bulk velocity (Q is flow rate), and ν is kinematic viscosity.

Figure 4 shows the relation between the Reynolds number Re_m and the friction factor λ for the smooth surface. The laminar theoretical relation[26] ($\lambda = 1.17 \times 64/\mathrm{Re}_m$) and the turbulent empirical relation[27] ($\lambda = 1.06 \times 0.3164 \times \mathrm{Re}_m^{-0.25}$), taking into account the channel-aspect ratio ($W/H^* = 4.67$ in the present study), are also indicated in the figure. The effective channel height H for the smooth surface was evaluated to be 30.7 mm in the laminar flow region for the glycerol-water mixture. Adopting this value, in the turbulent flow region of both working fluids, the data for the smooth surface agree well with the turbulent empirical relation.

Figure 5 shows the relation between the Reynolds number Re_m and the friction factor λ for the riblet surface. In the

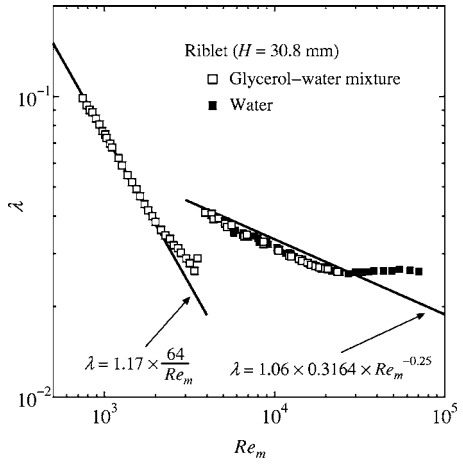

FIG. 5. Friction factor versus Reynolds number on the riblet surface.

turbulent flow region, the friction factor for the riblet surface is smaller than that for the smooth surface. The effective *channel height for the riblet surface was 30.8 mm, which indicates that the virtual origin of the riblet was located downward at a distance 0.07 times the riblet height from the top. This relationship agrees closely with that of a previous study.[12] The present experimental value (=0.07) is smaller than an analytical value[25] (=0.2) for a riblet with trapezoidal grooves of $s/h=1$ because the shapes of the riblet at the top are different.

Figure 6 shows the relation between the drag reduction ratio, DR and the nondimensional riblet height h^+, where the DR is defined as follows:

$$\mathrm{DR} = \frac{\lambda_{\mathrm{smooth}} - \lambda}{\lambda_{\mathrm{smooth}}} \times 100, \tag{2}$$

where $\lambda_{\mathrm{smooth}}$ is the friction factor on the smooth surface. Note that the DR is evaluated at the fixed Reynolds number Re_m, either at the fixed mass flow rate or the fixed pressure gradient,[28] since the equivalent diameter d_h depends on the surface configuration. The riblet height h^+ and lateral rib spacing s^+ are defined as follows:

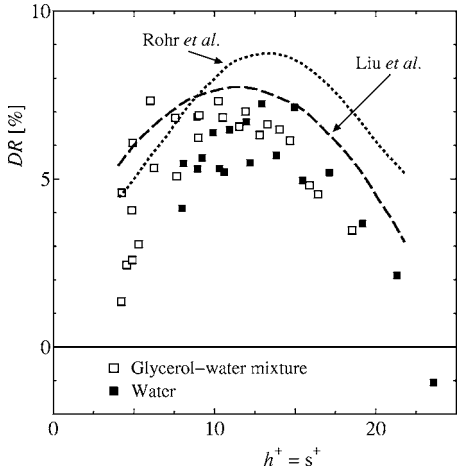

FIG. 6. Drag reduction versus riblet height in the wall unit.

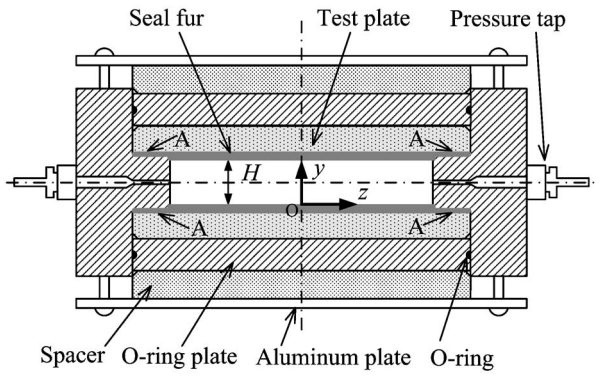

FIG. 7. Cross section of the rectangular duct for the seal fur surface.

$$h^+ = \frac{h\overline{u_\tau}}{\nu}, \quad s^+ = \frac{s\overline{u_\tau}}{\nu}, \tag{3}$$

where $\overline{u_\tau}$ is the mean friction velocity and is obtained by the measurement of the pressure loss for each test plate. It is found that the relation between DR and $h^+(=s^+)$ for the present riblet is comparable with the measurements[6,8] for the V-shaped riblet of $h/s=1$. Therefore, we may conclude that the present method of evaluating the effective channel height is also satisfactory for the riblet surface.

In the same manner as for the riblet surface, the effective channel height for the seal fur surface was evaluated, and the resultant value was $H=28.8$ mm, about 2 mm smaller than that (=30.7 mm) for the smooth surface, due to the flexibility of the seal fur surface. Figure 7 shows the cross section of the rectangular duct for the seal fur surface. The gray area represents the seal fur which was glued to the test plate. In the area between the test plates and the channel, represented by A in the figure, the seal fur surface is squashed, so the effective channel height for the seal fur surface is smaller than that for the smooth surface.

Figure 8 shows the distribution of the mean velocity U/U_c measured by the LDV system on the smooth and seal fur surfaces at the spanwise location $z/W=0.22$, and the Reynolds number $\mathrm{Re}_m=500$ for the glycerol-water mixture,

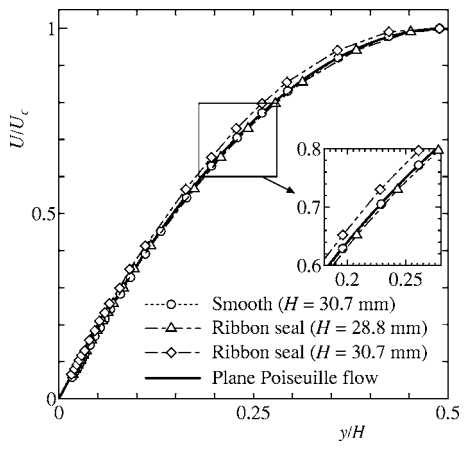

FIG. 8. Distribution of streamwise mean velocity at $z/W=0.22$, $\mathrm{Re}_m=500$ for the glycerol-water mixture.

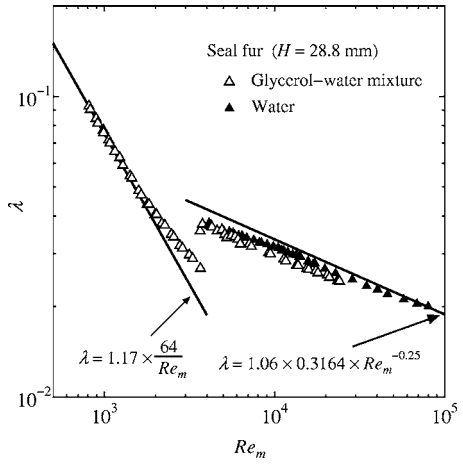

FIG. 9. Friction factor versus Reynolds number on the seal fur surface.

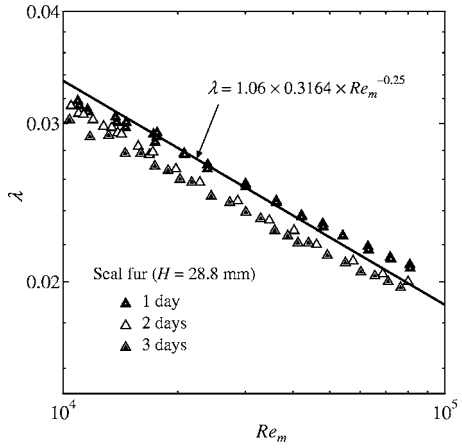

FIG. 10. Effect of residual air included in seal fur on relation between friction factor and Reynolds number for water.

where U_c is the mean velocity at the center of the channel ($y/H=0.5$). In the figure, the laminar theoretical mean velocity profile for the plane Poiseuille flow,

$$U = -\frac{1}{\mu}\frac{dP}{dx}(Hy - y^2), \tag{4}$$

is also presented, where dP/dx is the streamwise pressure gradient, and μ is the dynamic viscosity. To normalize the wall-normal distance from the test surface y, both $H=28.8$ mm and $H=30.7$ mm are used for the seal fur surface. The measured mean velocity profiles for the smooth surface and seal fur surface at $H=28.8$ mm agree well with the theoretical mean velocity profile, while the mean velocity U/U_c for the seal fur surface $H=30.7$ mm does not. Therefore, we can confirm the reliability of the present method of evaluating the effective channel height by using the laminar theoretical relation between Re_m and λ for the seal fur surface.

B. Friction factor and drag reduction ratio

Figure 9 shows the relation between the Reynolds number Re_m and the friction factor λ for the seal fur surface. It is found that drag reduction can be obtained by using the seal fur surface in the turbulent flow region. For the seal fur surface, unlike the riblet surface, a drag increase due to the effect of surface roughness does not appear even at the highest Reynolds number tested ($\mathrm{Re}_m=80\,000$), indicating that the range of Reynolds numbers where the drag reduction appears for seal fur is wider than that for riblets. The data of the seal fur surface for water do not agree with those for the glycerol-water mixture completely. It cannot reject the possibility that in the higher Reynolds number region the effective channel height for water was slightly different from that for the glycerol-water mixture. Note that the effective channel height H evaluated for glycerol-water mixture was also used for water, in which the pressure-loss measurements could not be performed correctly in the laminar flow region since the pressure loss was too small. Here, keeping the reference point of traversing device of the LDV system, we confirmed that the location of the seal fur surface (zero-velocity points on the mean velocity profiles) did not change in the laminar flow region ($\mathrm{Re}_m=500$) and the turbulent flow region ($\mathrm{Re}_m=7\,000$) for the glycerol-water mixture. This means that there was no effect of the absolute static pressure on the location of the seal fur surface.

To investigate the effect of the residual air included in seal fur surface on the friction factor λ, the relations between λ and Re_m for 1 day, 2 days, and 3 days after water is filled in the rectangular channel are shown in Fig. 10, where the effective channel height $H=28.8$ mm is used. The friction factor λ for after 1 day is larger than that for after 2 days at the same Reynolds number, which indicates that the amount of residual air is different, so that the effective channel height H is changed, and then the value of the friction factor λ is altered. However, λ for after 2 days agrees with that for after 3 days. Therefore, we may conclude that the effect of the residual air included in the seal fur surface on λ is negligible for more than after 2 days.

Figure 11 shows the variation in the drag-reduction ratio, DR with Reynolds number Re_m for the seal fur and riblet surfaces in glycerol-water mixture. The maximum DR for the seal fur surface is 12%, which is higher than that (DR=7.3%) for the riblet. In addition, it is noteworthy that

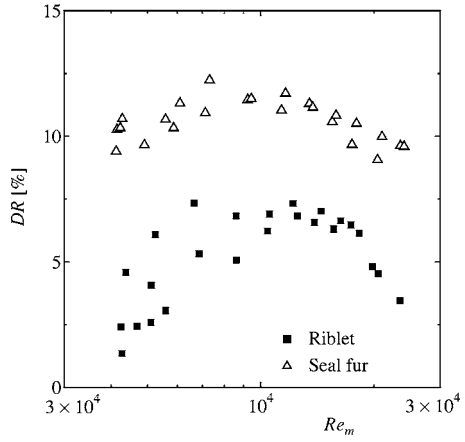

FIG. 11. Drag reduction ratios versus Reynolds number for the glycerol-water mixture.

(a)

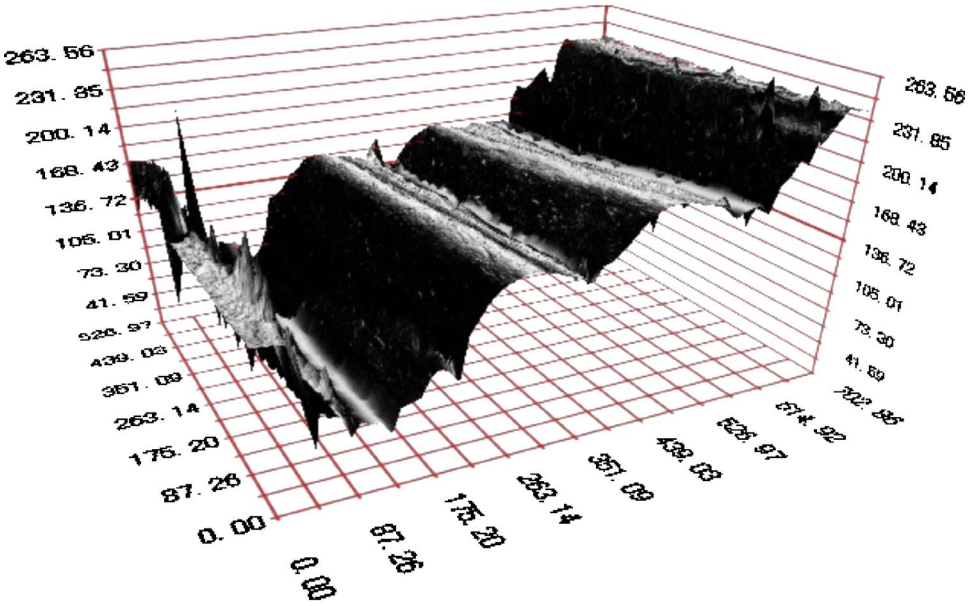

(b)

FIG. 12. Photograph of the seal fur surface: (a) two-dimensional (530 $\times$700 μm), (b) three-dimensional (unit, μm).

the Reynolds number range, where the DR is almost maximum for the seal fur surface, is much wider than that for the riblet surface.

C. Configuration of seal fur surface

Two-dimensional and three-dimensional photographs of the seal fur surface in a semiwet condition are shown in Figs. 12(a) and 12(b), respectively. The horizontal and vertical directions in Fig. 12(a) correspond to the spanwise and streamwise directions, respectively, while the horizontal and vertical directions in Fig. 12(b) correspond to the spanwise and wall-normal directions, respectively. The spanwise distribution of surface-roughness protrusion height for the seal fur surface is presented in Fig. 13. The root mean squared value of the surface-roughness protrusions h was $h'_{\mathrm{rms}}=36.7$ μm. Figures 12 and 13 show that the seal fur surface is comprised of complex and uneven shapes, compared to the riblet surface.

Figure 14 shows the power spectrum of the surface-roughness protrusions P_h for the seal fur surface. In the figure, the abscissa is the inverse of the spanwise wavelength $1/\lambda_h$, and the vertical dotted line represents the present riblet pitch $\lambda_h=0.7$ mm which corresponds to $\lambda_h^+=\lambda_h\overline{u_\tau}/\nu\simeq 7$ for the Reynolds number $\mathrm{Re}_m=7\,000$. This figure demonstrates that the roughness of the seal fur surface is comprised of various wavelengths. Several peaks for the seal fur surface appear around the riblet pitch ($0.2<\lambda_h<1.8$ mm, $2<\lambda_h^+$

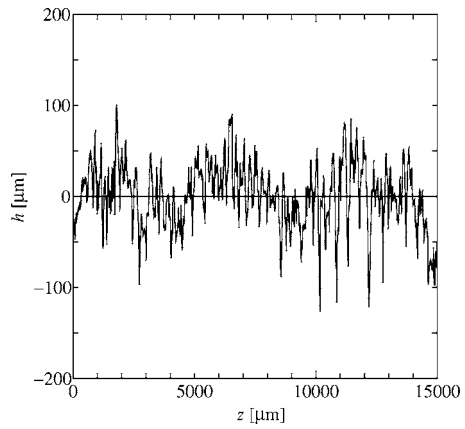

FIG. 13. Spanwise distribution of surface-roughness protrusion height for the seal fur surface.

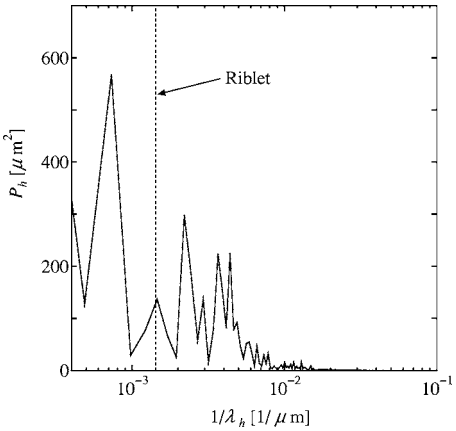

FIG. 14. Power spectrum of surface roughness protrusions for the seal fur.

<18 for $\mathrm{Re}_m=7\,000$). It can be deduced that, compared to the riblet surface having only a single wavelength, the uneven roughness with various wavelengths of the seal fur surface leads to a larger drag reduction ratio and a wider range of Reynolds numbers where drag reduction could be obtained (Fig. 11), and also to the absence of drag increase due to the effect of surface roughness even at the highest Reynolds number tested (Fig. 9).

D. Mean velocity and turbulence intensity

To clarify the effect of the secondary flow on velocity measurements, distributions of streamwise mean velocity U/U_c and turbulence intensity u'_{rms}/U_c at $z/W=0$ and $z/W=0.22$ for the smooth surface are shown in Fig. 15. Velocity

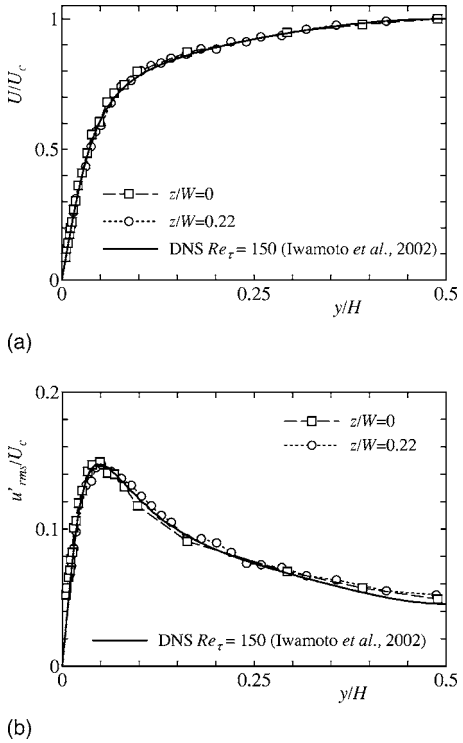

FIG. 15. Effect of secondary flow on velocity measurements for smooth surface at $z/W=0$ and $z/W=0.22$, $\mathrm{Re}_m=7\,000$ ($\mathrm{Re}_\tau=150$) for water: (a) streamwise mean velocity, (b) streamwise turbulence intensity.

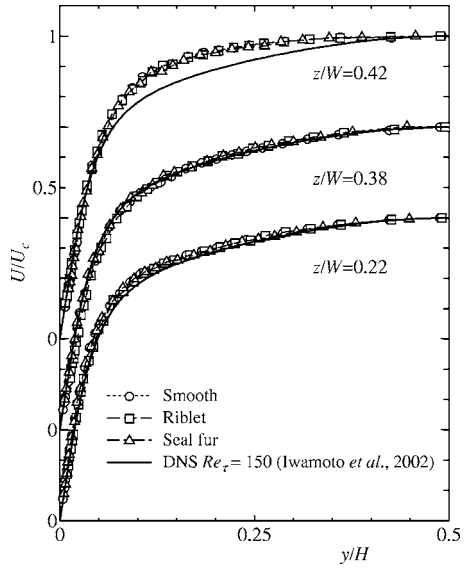

FIG. 16. Distribution of streamwise mean velocity at $\mathrm{Re}_m=7000$ for the glycerol-water mixture.

measurements for water were performed at the bulk Reynolds number $\mathrm{Re}_m=7\,000$ which corresponds to the friction Reynolds number $\mathrm{Re}_\tau=150$. The friction Reynolds number Re_τ is based on half the effective channel height $H/2$, mean friction velocity $\overline{u_\tau}$ obtained by the pressure loss, and kinematic viscosity ν:

$$\mathrm{Re}_\tau=\frac{(H/2)\overline{u_\tau}}{\nu}. \tag{5}$$

In the figure, the direct numerical simulation (DNS) data for the two-dimensional turbulent channel flow at $\mathrm{Re}_\tau=150$, computed by Iwamoto *et al.*,[29] are presented. The measurements of U/U_c and u'_{rms}/U_c at both $z/W=0$ and $z/W=0.22$ agree well with the corresponding DNS data, which indicates that the effect of the secondary flow is negligible at $z/W\leq 0.22$. We confirmed that at $z/W\leq 0.22$ the spanwise variation of the turbulence intensity at the center of the channel ($y/H=0.5$) was within the experimental uncertainty which was estimated to be $\pm 2\%$. As mentioned above, the effective channel height H on the seal fur surface was not evaluated for water, thus velocity measurements should be done for the glycerol-water mixture. Even if the effect of the secondary flow on turbulence statistics does not appear (see Fig. 15), it is better to measure velocity profiles at the center of the channel ($z/W=0$), taking into account the present aspect ratio. But we could not obtain the reliable data at $z/W=0$ for the glycerol-water mixture, because the sampling data rate of LDV measurements was much worse. Therefore, velocity measurements at $z/W\geq 0.22$ for the glycerol-water mixture are presented below.

Figure 16 shows the profiles of streamwise mean velocity U/U_c at $z/W=0.22$, 0.38, 0.42 for the smooth, riblet, and seal fur surfaces, respectively. Velocity measurements for glycerol-water mixture were performed at the bulk Reynolds number $\mathrm{Re}_m=7,000$. The mean velocity $z/W\leq 0.38$ almost agrees with the DNS data,[29] which indicates that the effect of the secondary flow on the mean velocity is negligible at

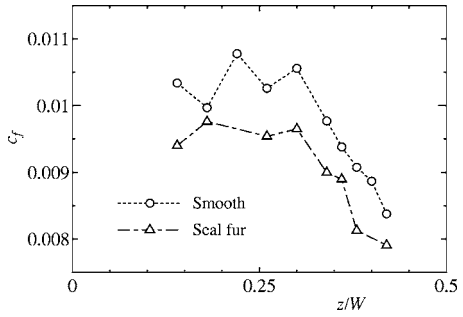

FIG. 17. Spanwise distribution of local skin friction coefficient on smooth and seal fur surfaces at Re_m=7 000 for the glycerol-water mixture.

$z/W \leq 0.38$ in the present channel flow with the aspect ratio $W/H^* = 4.67$, while U/U_c at $z/W = 0.42$ is larger due to the effect of the secondary flow. For $z/W = 0.22$, 0.38, and 0.42, the mean velocities for riblet and seal fur surfaces agree well with that for the smooth surface, which means that the effect of the secondary flow does not depend on the surface configuration used in the present experiment.

To investigate the drag-reducing effect on mean velocity and turbulence statistics, the inner scaling would be more advantageous than the outer scaling in many cases. However, we cannot use the mean friction velocity u_τ estimated by the pressure loss, since the local friction velocity u_τ varies with spanwise locations. Figure 17 shows the spanwise distribution of local skin friction coefficient c_f on smooth and seal fur surfaces at Re_m=7 000 for the glycerol-water mixture. The local skin friction coefficient c_f is defined as follows:

$$c_f = \frac{\tau_w}{\rho U_a^2/2}, \tag{6}$$

where τ_w is the wall shear stress and ρ is the density. The wall shear stress τ_w was obtained by the mean velocity gradient which was obtained by the least square approximation using mean velocity measurements (about seven points) at different y locations within the viscous sublayer ($y^+ = yu_\tau/\nu < 5$). The values of c_f for the seal fur surface are smaller than those for the smooth surface at any spanwise locations, which supports the drag-reducing ability of the seal fur surface. The spanwise variation of c_f for both smooth and seal fur surfaces is small for $z/W < 0.3$, although the data on c_f seem to be rather scattered. This indicates that the effect of secondary flow can be excluded for $z/W < 0.3$ in the present study. Here we checked that the difference between u_τ estimated by the mean velocity gradient and u_τ obtained by the Clauser method was not so large at the spanwise location $z/W = 0.22$ for the smooth surface. However the experimental uncertainty in u_τ was estimated to be ±5% of its absolute value, which was too large to compare turbulence statistics scaled on inner variables correctly. Moreover the Clauser method was not applicable to the seal fur and riblet surfaces.[12] Therefore, we used the outer scaling here for the mean velocity and turbulence statistics.

Distributions of streamwise turbulence intensity scaled by bulk velocity u'_{rms}/U_a are shown in Fig. 18, where ' represents the turbulent fluctuation with respect to the time average. The streamwise turbulence intensity u'_{rms}/U_a at $z/W = 0.22$ for the seal fur surface is about 5% smaller at $0.05 \leq y/H \leq 0.15$ than those for the smooth and riblet surfaces. At $z/W = 0.42$, the maximum for seal fur surface is about 6% smaller compared to the smooth surface, while the maximum for the riblet surface is about 3% smaller. The decrease in streamwise turbulence intensity is smaller than that of Suzuki and Kazagi[4] for the channel flow with the aspect ratio 10, probably because the riblet shape is different.

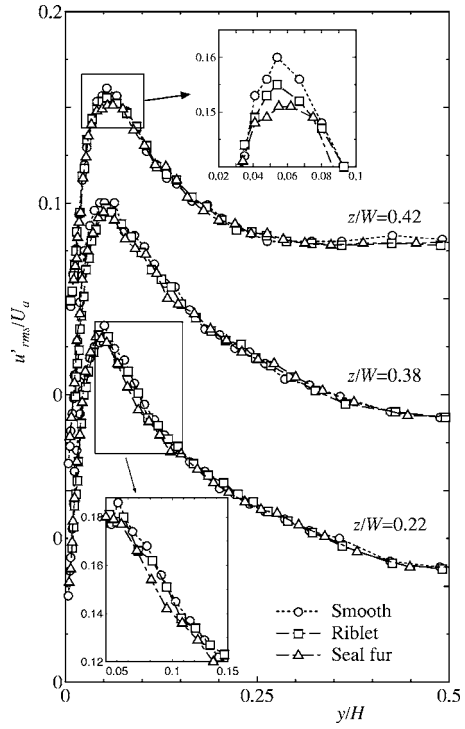

FIG. 18. Distribution of streamwise rms velocity fluctuation at Re_m=7 000 for the glycerol-water mixture.

IV. CONCLUSION AND DISCUSSION

The pressure loss for seal fur surface was precisely measured in a rectangular channel flow using a glycerol-water mixture even at the low-Reynolds number. The seal fur surface was measured by a three-dimensional laser microscope. The mean velocity and streamwise turbulence intensity were measured using an LDV system. The main results of the present study may be summarized as follows:

(1) The maximum drag reduction ratio for the seal fur surface is 12%, which is higher than that for the riblet surface. The Reynolds number range, where the drag-reduction ratio is remarkable for the seal fur surface, is much wider than that for the riblet surface. In addition, any drag increase due to the effect of surface roughness is not found up to the highest Reynolds number tested.

(2) In contrast to the riblet surface having only a single wavelength, the seal fur surface consists of uneven roughness with various wavelengths.

(3) The mean velocity profile scaled by the outer variable for the seal fur surface agrees with that for the smooth surface at any spanwise location. The streamwise turbulence

intensity for the seal fur surface is about 5% smaller than those for smooth and riblet surfaces.

The present study revealed that the seal fur surface had sufficient potential to provide a larger turbulent drag reduction in the wider Reynolds number region than riblets with only a single wavelength which are idealized models of shark skin. However, the other factors for drag reduction of seal fur surface, e.g., the effect of flexibility of the hair on the coherent structure in near-wall turbulence, the ability of direction rearrangement of fur surface to flow direction, and the difference in the hair between the hydrophilic and hydrophobic properties, should be also investigated to understand the physical mechanism causing the drag reduction. For this end, the experiments for the different kinds of seal fur surfaces may be helpful. In addition, the studies on the drag-reducing ability of artificial fur surface and the coating surface that has the same structure as the seal fur would be desired for the applications.

ACKNOWLEDGMENT

The measurements of seal fur surfaces performed at Yoshida Kikai Co., Ltd. using a 3D laser microscope (violet laser color 3D profile microscope, Keyence Co.) are gratefully acknowledged.

[1] M. J. Walsh, "Turbulent boundary layer drag reduction using riblets," AIAA Pap. 82-0169 (1982).
[2] M. J. Walsh, "Riblets as a viscous drag reduction technique," AIAA J. **21**, 485 (1983).
[3] M. J. Walsh and A. M. Lindemann, "Optimization and application of riblets for turbulent drag reduction," AIAA Pap. 84-0347 (1984).
[4] Y. Suzuki and N. Kasagi, "Turbulent drag reduction mechanism above a riblet surface," AIAA J. **32**, 1781 (1994).
[5] D. W. Bechert, M. Bruse, W. Hage, J. G. T. Van den Hoeven, and G. Hoppe, "Experiments on drag-reducing surfaces and their optimization with an adjustable geometry," J. Fluid Mech. **338**, 59 (1997).
[6] K. N. Liu, C. Christodoulou, O. Riccius, and D. D. Joseph,"Drag reduction in pipes lined with riblets," AIAA J. **28**, 1697 (1990).
[7] S. Nakao, "Application of V shape riblets to pipe flows," ASME Trans. J. Fluids Eng. **113**, 587 (1991).
[8] J. J. Rohr, G. W. Andersen, L. W. Reidy, and E. W. A. Hendricks, "Comparison of the drag-reducing benefits of riblets in internal and external flows," Exp. Fluids **13**, 361 (1992).
[9] P. Vukoslavčević, J. M. Wallace, and J.-L. Balint, "Viscous drag reduction using streamwise-aligned riblets," AIAA J. **30**, 1119 (1992).
[10] Y. P. Tang and D. G. Clark, "On near-wall turbulence-generating events in a turbulent boundary layer on ariblet surface," Appl. Sci. Res. **50**, 215 (1993).
[11] S.-R. Park and J. M. Wallace, "Flow alteration on drag reduction by riblets in turbulent boundary layer," AIAA J. **32**, 31 (1994).
[12] K.-S. Choi, "Near-wall structure of a turbulent boundary layer with riblets," J. Fluid Mech. **208**, 417 (1989).
[13] W. L. Keith, "Spectral measurements of pressure fluctuations on riblet," AIAA J. **27**, 1822 (1989).
[14] L. Djenidi and R. A. Antonia, "Laser Doppler anemometer measurements of turbulent boundary layer over a riblet surface," AIAA J. **34**, 1007 (1996).
[15] J.-J. Wang, S.-L. Lan, and G. Chen, "Experimental study on the turbulent boundary layer flow over riblets surface," Fluid Dyn. Res. **27**, 217 (2000).
[16] S.-J. Lee and S.-H. Lee, "Flow field analysis of a turbulent boundary layer over a riblet surface," Exp. Fluids **30**, 153 (2001).
[17] D. C. Chu and G. E. Karniadakis, "A direct numerical simulation of laminar and turbulent flow over riblet-mounted surfaces," J. Fluid Mech. **250**, 1 (1993).
[18] H. Choi, P. Moin, and J. Kim, "Direct numerical simulation of turbulent flow over riblets," J. Fluid Mech. **255**, 503 (1993).
[19] D. Goldstein, R. Handler, and L. Sirovich, "Direct numerical simulation of turbulent flow over a modelled riblet covered surface," J. Fluid Mech. **302**, 333 (1995).
[20] G. E. Karniadakis and K.-S. Choi, "Mechanisms on transverse motions in turbulent wall flows," Annu. Rev. Fluid Mech. **35**, 45 (2003).
[21] L. Sirovich and S. Karlsson, "Turbulent drag reduction by passive mechanisms," Nature (London) **388**, 753 (1997).
[22] D. W. Bechert, M. Bruse, and W. Hage, "Experiments with three-dimensional riblets as an idealized model of shark skin," Exp. Fluids **28**, 403 (2000).
[23] K. Koeltzsch, A. Dinkelacker, and R. Grundmann, "Flow over convergent and divergent wall riblets," Exp. Fluids **33**, 346 (2002).
[24] R. B. Dean, "Reynolds number dependence of skin friction and other bulk flow variables in two-dimensional rectangular duct flow," ASME Trans. J. Fluids Eng. **100**, 2153 (1978).
[25] D. W. Bechert and M. Bartenwerfer, "The viscous flow on surfaces with longitudinal ribs," J. Fluid Mech. **206**, 105 (1989).
[26] R. J. Cornish, "Flow in a pipe of rectangular cross section," Proc. R. Soc. London, Ser. A **120**, 691 (1928).
[27] I. E. Idelchik, *Handbook of Hydraulic Resistance* (Springer, Berlin, 1986), p. 87.
[28] H. Choi, P. Moin, and J. Kim, "On the effect of riblets in fully developed laminar channel flows," Phys. Fluids A **3**, 1892 (1991).
[29] K. Iwamoto, Y. Suzuki, and N. Kasagi, "Reynolds number effect on wall turbulence: toward effective feedback control," Int. J. Heat Mass Transfer **23**, 678 (2002).